C. R. Mecanique 347 (2019) 294–304

Contents lists available at ScienceDirect

Comptes Rendus Mecanique

www.sciencedirect.com

Patterns and dynamics: homage to Pierre Coullet / *Formes et dynamique : hommage à Pierre Coullet*

Quasipatterns versus superlattices resulting from the superposition of two hexagonal patterns

Structures quasi cristallines et super-réseaux résultant de la superposition de deux réseaux hexagonaux

Stéphan Fauve [a,*], Gérard Iooss [b]

[a] *Laboratoire de physique statistique, École normale supérieure, PSL Research University, UPMC Université Paris-6, Sorbonne Universités, Université Paris-Diderot, Sorbonne Paris-Cité, CNRS, 24, rue Lhomond, 75005 Paris, France*
[b] *Université Côte d'Azur, CNRS, LJAD, Parc Valrose 06108, Nice cedex 2, France*

ARTICLE INFO

Article history:
Received 28 August 2018
Accepted 9 November 2018
Available online 9 April 2019

Keywords:
Bifurcations
Asymptotic series
Quasicrystals
Instability in fluids
Small divisors

Mots-clés :
Bifurcations
Séries asymptotiques
Quasi-cristaux
Instabilité dans les fluides
Petits diviseurs

ABSTRACT

We present a short review of the experimental observations and mechanisms related to the generation of quasipatterns and superlattices by the Faraday instability with two-frequency forcing. We show how two-frequency forcing makes possible triad interactions that generate hexagonal patterns, twelvefold quasipatterns or superlattices that consist of two hexagonal patterns rotated by an angle α relative to each other. We then consider which patterns could be observed when α does not belong to the set of prescribed values that give rise to periodic superlattices. Using the Swift–Hohenberg equation as a model, we find that quasipattern solutions exist for nearly all values of α. However, these quasipatterns have not been observed in experiments with the Faraday instability for $\alpha \neq \pi/6$. We discuss possible reasons and mention a simpler framework that could give some hint about this problem.

RÉSUMÉ

Nous présentons une courte revue des observations expérimentales et des mécanismes qui ont permis d'engendrer des structures quasi cristallines à l'aide de l'instabilité de Faraday sous l'effet d'une excitation périodique comportant deux fréquences. Nous montrons comment l'excitation à deux fréquences permet d'obtenir des triades de vecteurs d'onde résonantes qui induisent la formation de structures hexagonales, de structures quasi cristallines dodécagonales ou de super-réseaux résultant de la superposition de deux réseaux d'hexagones tournés l'un par rapport à l'autre d'un angle α. Nous considérons ensuite quelles sont les structures obtenues lorsque α ne prend pas la série de valeurs discrètes conduisant à un super-réseau périodique. Nous montrons sur l'équation de Swift–Hohenberg qu'il existe dans ce cas des solutions à symétrie quasi cristalline pour presque toutes les valeurs de α. Nous discutons les raisons possibles pour lesquelles ces solutions

* Corresponding author.
E-mail addresses: fauve@lps.ens.fr (S. Fauve), iooss.gerard@orange.fr (G. Iooss).

https://doi.org/10.1016/j.crme.2019.03.006

n'ont pas été observées expérimentalement pour $\alpha \neq \pi/6$ et nous mentionnons un cadre plus simple qui permettrait d'éclaircir cette question.

1. Introduction

Pattern-forming instabilities have been studied in fluid mechanics since the 19th century. In 1831, Faraday observed that standing surface waves can be generated by vertically vibrating a fluid layer above a critical amplitude [1]. Linear stability analysis has been first used to understand the Kelvin–Helmholtz instability [2], i.e. waves amplified by a shear flow at the interface between two fluids of different densities. The first quantitative experimental studies on pattern-forming instabilities were carried out by Bénard in 1900 on thermal convection [3]. In contrast to the two first examples, patterns generated by the Bénard–Rayleigh instability are not standing or propagating waves, but stationary spatially periodic structures. In all these examples, pattern-forming instabilities are related to a transition from a spatially homogeneous (often motionless) state, to one varying periodically in space or time. Linear stability analysis of the homogeneous state provides the critical wave number k_c of the first unstable mode and the critical value of a control parameter for the instability threshold. It gives no information about the geometry of the pattern. Any superposition of linear modes with wave vectors $\mathbf{k}_p$ $(p = 1, ..., N)$ indeed provides a growing pattern above the instability threshold, provided $|\mathbf{k}_p| = k_c$. The geometry of the pattern is selected by the nonlinear interactions between the growing linear modes.

In the case of a fluid layer of infinite horizontal extent, the spatial dependence of linear modes is of the form $\exp(\pm i\,\mathbf{k}_p \cdot \mathbf{r})$ where $\mathbf{r} = (x, y)$. These modes can be superposed with arbitrary phases and amplitudes to give rise to an infinite number of growing patterns. Starting from Faraday [1], only a subclass of periodic patterns, periodic tilings of the plane, have been considered for more than one and a half century. As written by Chandrasekhar [4], "it may be reasonable to argue that since there are no points or directions in the horizontal plane which are preferred, the entire layer in the marginal state must be tessellated into regular polygons with the cell walls being surfaces of symmetry. Such complete symmetry will require that the polygons be either equilateral triangles, squares, or regular hexagons". Of course, one should also consider stripes or rolls, i.e. patterns that depend only on one space coordinate $(N = 2)$ and one could take into account parallelograms instead of squares. Considering patterns that consist of a unit cell that repeats itself regularly was certainly the same kind of simplification that prevailed in crystallography until the discovery of quasicrystals [5]. Shortly after this discovery, it has been observed that hydrodynamic instabilities can also generate more complex patterns than periodic tilings of the plane with regular polygons. A large variety of these patterns have been first observed using the Faraday instability, including not just periodic patterns of stripes, squares or hexagons, but many more complex patterns such as superlattices, quasipatterns, localized structures (oscillons).

1.1. Patterns generated by the Faraday instability

The Faraday instability is observed on the free surface of a vertically vibrated fluid layer. When the vibration is sinusoidal at angular frequency ω, a standing wave pattern with wavenumber k_c is generated above a critical vibration amplitude. k_c is related to ω. When viscous dissipation is not too large, it is given with a good approximation by the dispersion relation $\omega = 2\,\Omega(k)$ of gravity-capillary waves [6]. We have assumed that, as usual for parametric amplification, the standing waves that are amplified above the instability threshold are subharmonic, i.e. have a fundamental frequency $\omega/2$. However, in thin fluid layers for which bottom friction can be large, the harmonic response can have a lower threshold than the subharmonic one [7].

Early experiments performed in a container with a horizontal extension much larger than the instability wavelength displayed square patterns above the instability onset [8–10], in agreement with the observations of Faraday. These experiments were all performed in the capillary range with moderate viscous dissipation. When dissipation is increased, one-dimensional stripe patterns are observed [11,12]. Another important parameter is the relative contribution of gravity to surface tension in the dispersion relation. When it is tuned appropriately by changing ω, hexagons can be observed [13].

A qualitative explanation of the pattern selection process has been provided in [12]. It relies on a characteristic feature of the Faraday instability. Consider two standing wave patterns with wave vectors $\mathbf{k}_1$ and $\mathbf{k}_2$ and complex amplitudes A_1 and A_2. If $|\mathbf{k}_1| = |\mathbf{k}_2| = k_c$, both are neutral at the instability threshold. Quadratic nonlinear interactions of these modes give a standing wave of frequency ω and a wave vector $\mathbf{k}_1 + \mathbf{k}_2$ (see Fig. 1a). In the absence of dissipation, this mode is neutral if $\Omega(|\mathbf{k}_1 + \mathbf{k}_2|) = 2\,\Omega(k_c)$. This relation cannot be fulfilled if $\Omega(k)$ is concave, i.e. for pure gravity waves $(k_c \to 0)$. For pure capillary waves $(k_c \to \infty)$, it requires that the angle θ_r between $\mathbf{k}_1$ and $\mathbf{k}_2$ is such that $\cos(\theta_r/2) = 2^{-1/3}$ i.e. $\theta_r \approx 75\,\text{deg}$. When ω is decreased, k_c decreases and θ_r decreases to zero when $k_c l_c \to 1/\sqrt{2}$, where l_c is the capillary length. If viscous dissipation is small, this harmonic mode is weakly damped. To leading order, its amplitude B is governed by the equations

$$\dot{A}_1 = \mu A_1 - \overline{A_2} B + \cdots \tag{1}$$

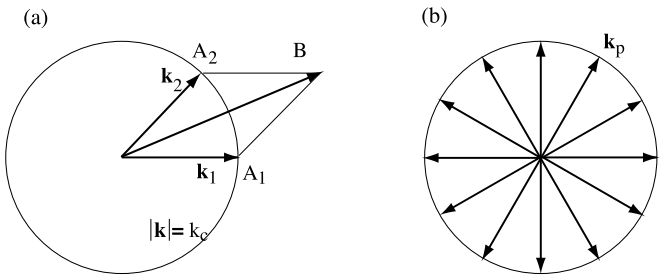

Fig. 1. (a) Two neutral modes with wave vectors $\mathbf{k}_1$ and $\mathbf{k}_2$ and amplitudes A_1 and A_2 oscillating at $\omega/2$, nonlinearly interact to give a wave with wave vector $\mathbf{k}_1+\mathbf{k}_2$ and amplitude B oscillating at ω. In the absence of dissipation, this wave is neutral if $\Omega(|\mathbf{k}_1+\mathbf{k}_2|)=2\Omega(k_c)=\omega$. (b) N neutral modes with wave vectors $\mathbf{k}_p$ at equal angles $2\pi/N$ on the circle $|\mathbf{k}_p|=k_c$.

$$\dot{A}_2=\mu A_2-\overline{A_1}B+\cdots \tag{2}$$

$$\dot{B}=-\nu B+2A_1A_2+\cdot \tag{3}$$

where an overbar stands for the complex conjugate, μ is the distance to threshold, and $\nu>0$ is related to damping. The relative signs and the coefficients of the quadratic nonlinearities are chosen to conserve energy in the absence of dissipation. In the presence of dissipation, $\nu\neq 0$, and B can be adiabatically eliminated, $B\approx 2A_1A_2/\nu$, giving a contribution to the cubic nonlinearities in the amplitude equations for A_k with a coefficient $-2/\nu$. When dissipation is small, neutral modes with wave vectors making an angle θ_r are therefore strongly inhibited due to the energy transferred to harmonic modes by triad interaction. Quantitative calculations have shown that this mechanism indeed selects the preferred pattern in the low dissipation case [14,15]. It has been found that the rotational order of the pattern increases when θ_r decreases to zero, with the selection of 8-fold, 10-fold, ... quasicrystalline patterns in good agreement with the experimental observations [16].

Another type of patterns observed with the Faraday instability in the case of a sinusoidal forcing consists of patterns displaying two length scales, a first one related to k_c together with a long wavelength modulation with wavenumber $K<k_c$ with K and k_c commensurate such that the pattern is periodic in space [17]. These patterns were later called superlattices (see below) and have been recently observed in direct numerical simulations [18].

1.2. The observation of quasipatterns with two-frequency forcing of the Faraday instability: triad interactions

We now present an efficient method that has been used to generate quasipatterns and superlattices using the Faraday instability. The idea of the method is to modify the forcing in order to allow triad interactions between neutral modes. These interactions are usually forbidden with sinusoidal forcing. Indeed, in the case of a fluid layer of infinite horizontal extent, the perturbation of the free surface is, according to Floquet's theory,

$$\xi(\mathbf{r},t)=\sum_{p=1}^{N}\left[A_p\exp(\mathrm{i}\,\mathbf{k}_p\cdot\mathbf{r})+\text{c.c.}\right]\left[\chi(t)\exp(\mathrm{i}\sigma\, t)+\text{c.c.}\right]+\cdots \tag{4}$$

where $\chi(t)$ is periodic with the period of the forcing $2\pi/\omega$ and $\mathrm{i}\sigma$ is the Floquet exponent (see Fig. 1b). The dots stand for higher-order terms generated by the nonlinearities of the problem above the instability threshold. If the response is subharmonic, $\sigma=\omega/2$. Therefore, the unstable solution (4) spontaneously breaks the invariance $t\to t+2\pi/\omega$ of the forcing. Consequently, if $\xi(\mathbf{r},t)$ is a bifurcated solution, $\xi(\mathbf{r},t+2\pi/\omega)=-\xi(\mathbf{r},t)$ is another solution. This implies that the amplitude equation for A_p should be invariant under the transformation $A_p\to -A_p$, thus forbidding quadratic nonlinearities of the form

$$\frac{\partial A_p}{\partial t}=\mu A_p+\lambda\overline{A}_q\overline{A}_r+\cdots \tag{5}$$

This can also be understood from resonance arguments. Spatial resonance is fulfilled provided that $\mathbf{k}_p+\mathbf{k}_q+\mathbf{k}_r=0$. A_p is related to an oscillation at angular frequency $\omega/2$, whereas $\overline{A}_q\overline{A}_r$ corresponds to $-\omega$, therefore temporal resonance is not satisfied and λ should vanish.

The first motivation to use a two-frequency periodic forcing was to allow quadratic nonlinearities and therefore triad interactions by changing the temporal symmetries of the problem [19]. A two-frequency periodic forcing can be written

$$f(t)=a\left[\cos\theta\,\cos m\omega t+\sin\theta\cos(n\omega t+\phi)\right] \tag{6}$$

where $a\cos\theta$ (respectively $a\sin\theta$) is the amplitude of the component at angular frequency $m\omega$ (respectively $n\omega$). m and n are co-prime integers, therefore $f(t)$ is periodic with period $2\pi/\omega$. The phase difference can be taken such that $0\le\phi\le 2\pi/m$ using Bezout's theorem. If m and n have different parities, the most unstable resonance tongue can be harmonic ($\sigma=\omega$), therefore quadratic nonlinearities are allowed in (5). This can be easily understood if the component with

$m = 2$ is slightly perturbed by the component with $n = 3$. The response of the surface is at angular frequency $m\omega/2 = \omega$ (subharmonic response to the dominant forcing component), but the angular frequency of the forcing is also ω. The resonance argument can be also used: A_p (respectively $\overline{A_q}\overline{A_r}$) in (5) are related to an angular frequency $m\omega/2 = \omega$ (respectively -2ω). The angular frequency $n\omega = 3\omega$ now involved in λ fulfills temporal resonance. Triad interactions that result from quadratic nonlinearities generate an hexagonal pattern [19], except for a particular value of ϕ for which λ vanishes [12]. More generally, quadratic nonlinearities are allowed when a component of the forcing with m even is perturbed by another component with n odd.

The second motivation to use a two-frequency periodic forcing was to generate unstable modes with two different wavenumbers $|\mathbf{k^{(m)}}| = \mathbf{k}_c$ and $|\mathbf{k^{(n)}}| = \mathbf{k}_d$ respectively related to the forcing frequencies $m\omega$ and $n\omega$ through the dispersion relation of the Faraday instability. If modes with wave vectors k_c bifurcate first, and modes with wave vectors k_d are weakly damped, we expect resonant interactions between neutral and damped modes to select particular angles between neutral modes with a mechanism similar to the one described above in the case of sinusoidal forcing. A similar mechanism was used to model quasicrystals using a mean-field approach in the spirit of Landau [20]. In order to get neutral modes $\mathbf{k^{(m)}}$ and weakly damped modes $\mathbf{k^{(n)}}$, we need to work in the vicinity of the codimension-two bifurcation for which both sets of modes become simultaneously unstable. This selects the values of a and θ in (6) and therefore strongly reduces the number of free parameters of the forcing.

The method therefore consists in choosing an even–odd (m, n) couple in order to allow triad interactions between neutral modes. When the modes $\mathbf{k_n}$ bifurcate first, the response is subharmonic and triad interactions are forbidden. When the fluid viscosity is large, we get a pattern of stripes ($N = 2$). When the modes $\mathbf{k^{(m)}}$ bifurcate first with $\mathbf{k^{(m)}} = \mathbf{k}_c$, the response is harmonic and triad interactions generate a hexagonal pattern. We then move close to the codimension-two point. Changing the value of the remaining free parameter ϕ in Eq. (6) allows the observation of twelvefold quasipatterns. Therefore, to the leading order, these patterns can be understood as the superposition of two hexagonal patterns rotated one respect to the other by an angle $\alpha = \pi/6$. They have been observed in a small interval of ϕ but on a large range of frequency ω for $(m, n) = (4, 5), (4, 7), (6, 7), (8, 9)$ but not for $(m, n) = (2, 3)$. They can bifurcate from the flat surface, from an hexagonal pattern or from the pattern of stripes generated by the $n\omega$ component. In the hysteresis region between quasipatterns and the flat surface, one or several localized axisymmetric waves, sometimes called oscillons, have been also observed [12].

1.3. Theoretical models

Early theoretical models of the Faraday instability were performed in the limit of an inviscid fluid, dissipation being added in a phenomenological way [21]. This approach predicts a square pattern in the capillary regime [22] but does not capture the other patterns observed in different parameter ranges. A better controlled low-viscosity quasipotential approximation [14] is in better agreement with experiments in the small dissipation range. A weakly nonlinear analysis close to the instability threshold using the Navier–Stokes equation with finite viscosity displays a very good agreement with experiments [15]. Both the quasipotential approximation and the finite viscosity analysis have confirmed the observation of quasipatterns using sinusoidal forcing [16] and the quasipotential approximation has been used to model some experimental results with two-frequency forcing. Another approximation of the full Navier–Stokes equation that can be performed for finite viscosity in the case of a thin fluid layer is the inertial lubrication approximation [23]. It is the appropriate limit to get a possible competition between harmonic and subharmonic responses of the waves [7]. In the vicinity of the codimension-two bifurcation, for which both the harmonic response and the subharmonic one become simultaneously unstable, two subharmonic neutral modes with wave vectors making an appropriate angle are resonant with an harmonic mode. This can lead to the generation of a quasipattern [24].

A different theoretical approach used model equations of the Swift–Hohenberg type, i.e. nonlinear partial differential equations for scalar fields $u(x, y, t)$ that display a stationary pattern-forming instability at finite wavenumber. This approach obviously cannot provide a quantitative description of the Faraday problem, but it emphasizes the qualitative mechanisms for the generation of quasipatterns for any stationary pattern-forming instability. Il has been first shown that modifying the form of the cubic nonlinearity of the Swift–Hohenberg equation by considering terms involving more and more spatial derivatives allows one to generate patterns with an increasing rotational order [25]. This looks like a rather artificial model, but shows that two length scales are not generally required to generate quasipatterns, as is the case of the Faraday instability.

Models involving two length-scales, i.e. two wavenumbers k_c and k_d that become unstable for similar values of the forcing parameter, were studied in detail. This can be done either by taking two coupled Swift–Hohenberg-type equations, respectively for $u_1(x, y, t)$ and $u_2(x, y, t)$, displaying an instability at wavenumber k_c, respectively k_d [25], or one Swift–Hohenberg type equation for $u(x, y, t)$ with a linear part involving higher spatial derivatives, such that two wavenumbers k_c and k_d becomes simultaneously unstable [26]. In both cases, k_c and k_d can be related to the wavenumbers resulting from the forcing at angular frequency $m\omega$ (respectively $n\omega$). As explained above, one needs (m, n) even–odd to get quadratic nonlinearities in the amplitude equation, i.e. three-wave resonances. This can be achieved easily in both models if quadratic nonlinearities are taken into account in the Swift–Hohenberg-type equations. Then, if two wave vectors of modulus k_c separated by an angle θ_r become first unstable, they can be coupled through resonant three-wave interactions with a weakly damped wave vector of modulus k_d. The ratio k_d/k_c selects the value of θ_r through the relation $k_d/k_c = 2\sin(\theta_r/2)$ and therefore affects the rotational order of the pattern with wave vectors of modulus k_c. Depending on the nature of three-

wave interactions, this can be done either by inhibiting the pattern with two wave vectors separated by an angle θ or enhancing this configuration. This mechanism has been studied in detail for the two-frequency Faraday forcing with different values of m, n and many experimental observations have been found in agreement with theoretical predictions [27–29]. Coupled Swift–Hohenberg type equations have been also used to predict random patterns at the instability onset [30].

Although weakly nonlinear theory used to find the amplitude equations for N wave vectors distributed equally around a circle fairly well describes the experimental observations of quasipatterns ($N \geq 8$) and provides the correct mechanisms to explain their stability, it has been observed that the series is divergent because of the small divisor problem [31], [32]. Some modes generated by the nonlinear interactions between the neutral ones can have a wave vector arbitrary close to the neutral circle and therefore be close to resonance. This leads to large coefficients in the amplitude equation when they are adiabatically eliminated. This problem primarily concerns the existence of quasipatterns described as power series of the bifurcation parameter whatever the stability of these quasipatterns with respect to other planforms. It has been studied on the Swift–Hohenberg equation, although quasipatterns are not stable in that equation. It has been found that the divergent series can be used to build a quasiperiodic solution, which is an approximation of a solution to the Swift–Hohenberg equation [32,33], and this also holds for quasipatterns in the Bénard–Rayleigh steady convection [34].

1.4. Superlattices

As mentioned above, the Faraday instability can also generate patterns displaying two length scales, a first one related to the forcing frequency together with a long wavelength modulation. These length scales being commensurate, the pattern is periodic in space [17]. A variety of such patterns have been observed with two-frequency forcing [35–37] and have been called superlattices. Different types of superlattices have been reported: some of them bifurcate rather far from the codimension-two point for which quasipatterns are observed and involve a subharmonic frequency $m\omega/4$ together with a slow spatial modulation. Others bifurcate close to the codimension-two point and, therefore, could be in competition with quasipatterns. As said above, these quasipatterns can be understood as the superposition of two hexagonal patterns with wavenumber k_c, rotated by an angle $\alpha = \pi/6$ relative to each other. Among the superlattices found close to the codimension-two point, some of them result from two hexagonal patterns with $0 < \alpha < \pi/6$. It has been shown that, for some particular values of α, the resulting pattern is periodic and spanned by two wave vectors $\mathbf{K_1}$ and $\mathbf{K_2}$ with modulus K and making an angle $2\pi/3$ [38]. The hexagonal patterns are given by $\{\mathbf{k_1}, \mathbf{k_2}\}$, respectively $\{\mathbf{k'_1}, \mathbf{k'_2}\}$. We have $\mathbf{k_1} = p\,\mathbf{K_1} + q\,\mathbf{K_2}$, $\mathbf{k'_1} = p\,\mathbf{K_1} + (p-q)\,\mathbf{K_2}$, where p and q are co-prime integers such that $p > q > p/2 > 0$ and $p+q$ is not a multiple of 3. The angles α for superlattices are given by

$$\cos\alpha = \frac{p^2 + 2\,p\,q - 2\,q^2}{2(p^2 - p\,q + q^2)}, \quad \sin\alpha = \frac{\sqrt{3}p(p-2q)}{2(p^2 - pq + q^2)} \tag{7}$$

and $K = k_c/\sqrt{p^2 - pq + q^2}$. These superlattices are periodic structures, but involve two scales $2\pi/k_c$ and $2\pi/K$. The wavenumber k_d of the damped modes being a linear combination of $\mathbf{K_1}$ and $\mathbf{K_2}$, one can expect that it plays an important role in the stability of superlattices. Superlattices with different values of α or of (p, q) have been observed in the vicinity of the codimension-two point [37]. Their relative stability can be changed under the action of a third forcing frequency.

Although both these superlattices and quasipatterns can bifurcate from an hexagonal pattern close to the codimension-two point, the possible competition between superlattices and quasipatterns has not been investigated so far. A first question, simpler than the relative stability of these patterns, is related to the nature of the patterns that exist for nearly all values of α that do not correspond to superlattices. The next section is devoted to this problem.

2. Quasipattern solutions to the Swift–Hohenberg equation for arbitrary values of α

We look for quasipatterns, solutions to the steady Swift–Hohenberg PDE model equation

$$(1+\Delta)^2 u - \mu\,u + u^3 = 0 \tag{8}$$

where $u(x, y)$ is a real function of $(x, y) \in \mathbb{R}^2$, Δ is the Laplace operator, μ a real bifurcation parameter. In the Fourier plane, we have two pairs of six basic wave vectors $\{\mathbf{k}_j : j = 1, 2, ..6\}$ and $\{\mathbf{k}'_j; j = 1, 2, ..., 6\}$ both equally spaced on the unit circle (angle $\pi/3$ between $\mathbf{k}_j$ and $\mathbf{k}_{j+1}$ and between $\mathbf{k}'_j$ and $\mathbf{k}'_{j+1}$) and such that $\mathbf{k}_1$ is parallel to the x axis, while $\mathbf{k}'_1$ makes an angle $\alpha \leq \pi/6$ with the x axis (see Fig. 2). The quasilattice Γ is then defined by

$$\Gamma = \{\mathbf{k} \in \mathbb{R}^2; \mathbf{k} = \sum_{j=1,...6} m_j\mathbf{k}_j + m'_j\mathbf{k}'_j,\ m_j, m'_j \in \mathbb{N}$$

Notice that $\mathbf{k}_{j+3} = -\mathbf{k}_j$, $\mathbf{k}'_{j+3} = -\mathbf{k}'_j$ for $j = 1, 2, 3$, and notice that we also have

$$\mathbf{k}_1 - \mathbf{k}_2 + \mathbf{k}_3 = 0, \quad \mathbf{k}'_1 - \mathbf{k}'_2 + \mathbf{k}'_3 = 0$$

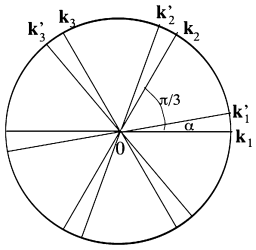

Fig. 2. Definition of the lattice Γ.

There are values of α for which Γ is periodic, as this is noticed in [38]. In particular, we obtain a hexagonal lattice in the case when Γ is a sublattice of a periodic lattice, built from two basic wave vectors $\mathbf{K_1}$ and $\mathbf{K_2}$ as mentioned above (see Eq. (7)).

This leads to the following definition.

Définition 2.1. The set $\mathcal{E}_p$ of special angles is defined as

$$\mathcal{E}_p := \{\alpha \in \mathbb{R}/2\,\pi\,\mathbb{Z};\, \cos\alpha \in \mathbb{Q}, \cos(\alpha + \pi/3) \in \mathbb{Q}\}$$

It is then clear that $\mathcal{E}_p$ contains the angles α that satisfy (7). Moreover, we have the following lemma.

Lemma 2.1. *The set $\mathcal{E}_p$ has a zero measure in $\mathbb{R}/2\,\pi\,\mathbb{Z}$.*

(i) If the wave vectors $\mathbf{k}_1$, $\mathbf{k}_2$, $\mathbf{k}'_1$, $\mathbf{k}'_2$ are not independent on $\mathbb{Q}$, then $\alpha \in \mathcal{E}_p$.

(ii) If $\alpha \in \mathcal{E}_p$ then the lattice Γ is periodic with an hexagonal symmetry, and wave vectors $\mathbf{k}_1$, $\mathbf{k}_2$, $\mathbf{k}'_1$, $\mathbf{k}'_2$ are combinations of only two smaller vectors, of equal length making an angle $2\,\pi/3$.

This lemma is proved in [39].

Let us assume that $\alpha \in \mathcal{E}_{qp} = (\mathcal{E}_p)^c$ (complement of $\mathcal{E}_p$). The function $u(x, y)$ is a real function that we put under the form of a Fourier expansion

$$u = \sum_{\mathbf{k}\in\Gamma} u^{(\mathbf{k})} e^{i\,\mathbf{k}\cdot\mathbf{x}},\ u^{(\mathbf{k})} = \overline{u}^{(-\mathbf{k})} \in \mathbb{C} \tag{9}$$

We observe that any $\mathbf{k} \in \Gamma$ may be written as

$$\mathbf{k} = z_1\mathbf{k}_1 + z_2\mathbf{k}_2 + z_3\mathbf{k}'_1 + z_4\mathbf{k}'_2,\ \ \mathbf{z} = (z_1, z_2, z_3, z_4) \in \mathbb{Z}^4$$

so that Γ spans a 4-dimensional vector space on $\mathbb{Q}$ since $\alpha \notin \mathcal{E}_p$. The norm $N_{\mathbf{k}}$ is defined by

$$N_{\mathbf{k}} = \sum_{j=1,\ldots,4} |z_j| = |\mathbf{z}|$$

To give a meaning to the above Fourier expansion, we need to introduce Hilbert spaces $\mathcal{H}_s$, $s \geq 0$:

$$\mathcal{H}_s = \left\{ u = \sum_{\mathbf{k}\in\Gamma} u^{(\mathbf{k})} e^{i\mathbf{k}\cdot\mathbf{x}};\, u^{(\mathbf{k})} = \overline{u}^{(-\mathbf{k})} \in \mathbb{C},\ \sum_{\mathbf{k}\in\Gamma} |u^{(\mathbf{k})}|^2 (1 + N_{\mathbf{k}}^2)^s < \infty \right\}$$

$\mathcal{H}_s$ is an algebra for $s > 2$, and possesses the usual properties of Sobolev spaces H_s in dimension 4. The following useful results are proved in [39].

Lemma 2.2. *If $\alpha \in \mathcal{E}_{qp}$, a function defined by a convergent Fourier series as (9) represents a quasipattern, i.e. is quasiperiodic in all directions.*

Lemma 2.3. *For nearly all $\alpha \in (0, \pi/6)$, in particular for $\alpha \in \mathcal{E}_{\mathbb{Q}} = \mathbb{Q}\,\pi \cap]0, \pi/6]$, the only solutions to $|\mathbf{k}(\mathbf{z})| = 1$ are $\pm\mathbf{k}_j$, $\pm\mathbf{k}'_j$ $j = 1, 2$ and $\mathbf{k} = \pm\mathbf{k}_3$, or $\pm\mathbf{k}'_3$, i.e. corresponding to $\mathbf{z} = (\pm 1, \mp 1, 0, 0)$ or $(0, 0, \pm 1, \mp 1)$.*

Let us denote by $\mathcal{E}_0$ the set of α's such that Lemma 2.3 applies.

Now, the following Lemma, proved also in [39], shows that inverting the operator $(1 + \Delta)^2$ gives rise to a small divisor problem. This is the source of the main difficulties of the problem, which needs the use of the strong implicit function theorem to be solved (see [39]).

Lemma 2.4. *For nearly all $\alpha \in \mathcal{E}_{qp} \cap (0, \pi/6)$, and for $\varepsilon > 0$, there exists $c > 0$ such that, for all $\mathbf{z} \neq 0$, such that $|\mathbf{k}(\mathbf{z})| \neq 1$, we have*

$$(|\mathbf{k}(\mathbf{z})|^2 - 1)^2 \geq \frac{c}{|\mathbf{z}|^{12+\varepsilon}} \tag{10}$$

Remark 1. In the case when $\alpha \in \mathcal{E}_p$, then by Lemma 2.1 the lattice is periodic and we have a much better estimate for a certain $c > 0$:

$$(|\mathbf{k}(\mathbf{z})|^2 - 1)^2 \geq c, \text{ for any } \mathbf{k} \in \Gamma \text{ with } |\mathbf{k}(\mathbf{z})| \neq 1$$

Below, we compute a formal expansion in powers of an amplitude ε. Such an expansion will diverge in general (Gevrey series). Once truncated, this expansion plays the role of a first approximation, and is a starting point of the Newton iteration process, ruling the Nash–Moser method used in [39].

2.1. Symmetries

Our problem possesses important symmetries. First, the symmetry $\mathbf{S}$ defined by $\mathbf{S}u = -u$, which commutes with (8) because of the imparity of the equation. Let us define $\mathbf{L}_0 = (1 + \Delta)^2)$, then we have $\mathbf{S}\mathbf{L}_0 = \mathbf{L}_0\mathbf{S}$, $\mathbf{S}u^3 = (\mathbf{S}u)^3$.

The system is invariant under rotations of the plane. Denoting by $\mathbf{R}_\theta$ the rotation of angle θ, centered at the origin, we define classically $(\mathbf{R}_\theta u)(\mathbf{x}) = u(\mathbf{R}_{-\theta}\mathbf{x})$, so that $\mathbf{R}_\theta\mathbf{L}_0 = \mathbf{L}_0\mathbf{R}_\theta$, $\mathbf{R}_\theta u^3 = (\mathbf{R}_\theta u)^3$.

The third symmetry $\boldsymbol{\tau}$ represents the symmetry with respect to the bisectrix of wave vectors $\mathbf{k}_1$ and $\mathbf{k}'_1$. This changes $(\mathbf{k}_1, \mathbf{k}_2, \mathbf{k}_3, -\mathbf{k}_1, -\mathbf{k}_2, -\mathbf{k}_3)$ into $(\mathbf{k}'_1, -\mathbf{k}'_3, -\mathbf{k}'_2, -\mathbf{k}'_1, \mathbf{k}'_3, \mathbf{k}'_2)$. We also have the commutation properties

$$\boldsymbol{\tau}\boldsymbol{L}_0 = \mathbf{L}_0\boldsymbol{\tau}, \ \boldsymbol{\tau}u^3 = (\boldsymbol{\tau}u)^3 \tag{11}$$

2.2. Formal series

We are looking for solutions, *invariant under rotations of angle* $\pi/3$, under the form of formal power series in an amplitude ε:

$$u = \sum_{n\geq 1} \varepsilon^n u_n, \ \mu = \sum_{n\geq 1} \varepsilon^n \mu_n$$

where ε is defined by the choice of u_1, and u_n has the form of a Fourier series (9) that is finite. At order ε, we obtain classically $\mathbf{L}_0 u_1 = 0$, which means that u_1 lies in the kernel of $\mathbf{L}_0$. In the class of functions invariant under the rotation of angle $\pi/3$, and provided that $\alpha \in \mathcal{E}_0$, the kernel is *two dimensional*, spanned by

$$v = \sum_{j=1,2,..,6} e^{i\mathbf{k}_j\cdot\mathbf{x}}, \ \ w = \sum_{j=1,2,..,6} e^{i\mathbf{k}'_j\cdot\mathbf{x}}$$

We observe that

$$\boldsymbol{\tau}v = w, \ \boldsymbol{\tau}w = v \tag{12}$$

We then set

$$u_1 = w + \beta_1 v \tag{13}$$

where the coefficient in front of w fixes the choice of the scale ε, provided that we choose to impose

$$\langle u_n, w\rangle = 0, \ \ n = 2, 3, \ldots \text{ where } \langle u, u'\rangle = \sum_{\mathbf{k}\in\Gamma} u^{(\mathbf{k})}\overline{u'}^{(\mathbf{k})}$$

since the linear operator $\mathbf{L}_0$ is selfadjoint in $\mathcal{H}_0$. The coefficient β_1 is chosen later. Then we can prove the following theorem.

Theorem 2.5. *Let us consider the Swift–Hohenberg model PDE (8). The superposition of two hexagonal patterns, differing by a small rotation of angle α leads to formal expansions in powers of an amplitude ε, of new bifurcating patterns invariant under rotations of angle $\pi/3$. For $\alpha \in \mathcal{E}_0$, we only have the bifurcating (classical) periodic hexagonal patterns and two branches of new patterns (see Fig. 5), with formal expansions of the form*

$$\begin{aligned} u &= \varepsilon(w + \beta_1 v) + \varepsilon^3\widetilde{u_3} + \ldots\varepsilon^{2n+1}\widetilde{u_{2n+1}} + .., \ \ \beta_1 = \pm 1 \\ \langle\widetilde{u_{2n+1}}, v\rangle &= \langle\widetilde{u_{2n+1}}, w\rangle = 0, \ \boldsymbol{\tau}\widetilde{u_{2n+1}} = \beta_1\widetilde{u_{2n+1}}, \ \boldsymbol{\tau}u = \beta_1 u \\ \mu &= \varepsilon^2\mu_2 + \varepsilon^4\mu_4 + \ldots + \varepsilon^{2n}\mu_{2n} + .., \ \mu_2 > 0 \end{aligned} \tag{14}$$

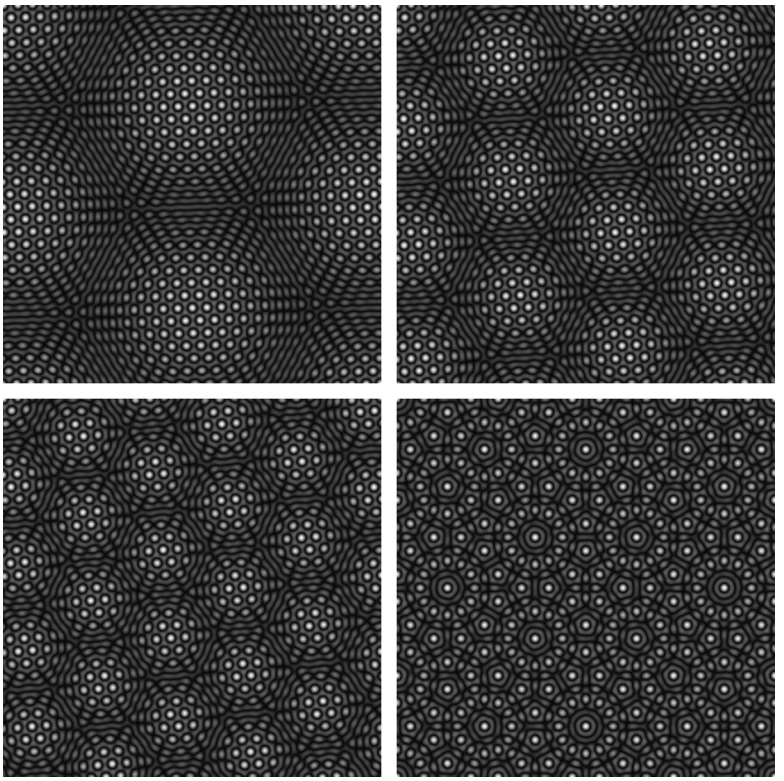

Fig. 3. Superposition of two hexagonal patterns for $\alpha = 4°, 7°, \pi/18, \pi/6$. Order ε and $\beta_1 = 1$ in Theorem 2.5 is represented.

$$v = \sum_{j=1,2,..,6} e^{i\,\mathbf{k}_j\cdot\mathbf{x}}, \quad w = \sum_{j=1,2,..,6} e^{i\,\mathbf{k}'_j\cdot\mathbf{x}}$$

For $\varepsilon \in \mathcal{E}_p \cap \mathcal{E}_0$, the expansions (14) converge, giving periodic patterns with hexagonal symmetry (superhexagons indicated in [38] and [37]).

Remark 2. We show in Figs. 3 and 4 the order ε of the bifurcating branches with $\beta_1 = 1$ and $\beta_1 = -1$ respectively, for different values of α.

Proof. At order ε^2, we obtain $\mathbf{L}_0 u_2 = \mu_1 u_1$, and the compatibility condition gives that there exists $\beta_2 \in \mathbb{R}$ such that

$$\mu_1 = 0,\ u_2 = \beta_2 v \tag{15}$$

Order ε^3 then leads to $\mathbf{L}_0 u_3 = \mu_2 u_1 - u_1^3$, with the compatibility conditions

$$a\,\mu_2 - c - 3\,b\,\beta_1^2 = 0$$
$$a\,\beta_1\mu_2 - 3\,b\,\beta_1 - c\,\beta_1^3 = 0$$

where

$$a = \langle v, v\rangle = \langle w, w\rangle = 6$$
$$b = \langle v^2 w, w\rangle = \langle w^2 v, v\rangle = 36$$
$$c = \langle w^3, w\rangle = \langle v^3, v\rangle = 90$$
$$\langle v^2 w, v\rangle = \langle w^2 v, w\rangle = \langle v^3, w\rangle = \langle w^3, v\rangle = 0$$

For example, the term $\langle w^3, v\rangle$ is 0 because there does not exist $m'_1, m'_2 \in \mathbb{Z}$ such that $m'_1\mathbf{k}'_1 + m'_2\mathbf{k}'_2 = \mathbf{k}_j$, due to Lemma 2.3, for $\alpha \in \mathcal{E}_0$. This gives

$$(c - 3\,b)(\beta_1^3 - \beta_1) = 0 \tag{16}$$

and there exists $\beta_3 \in \mathbb{R}$ such that

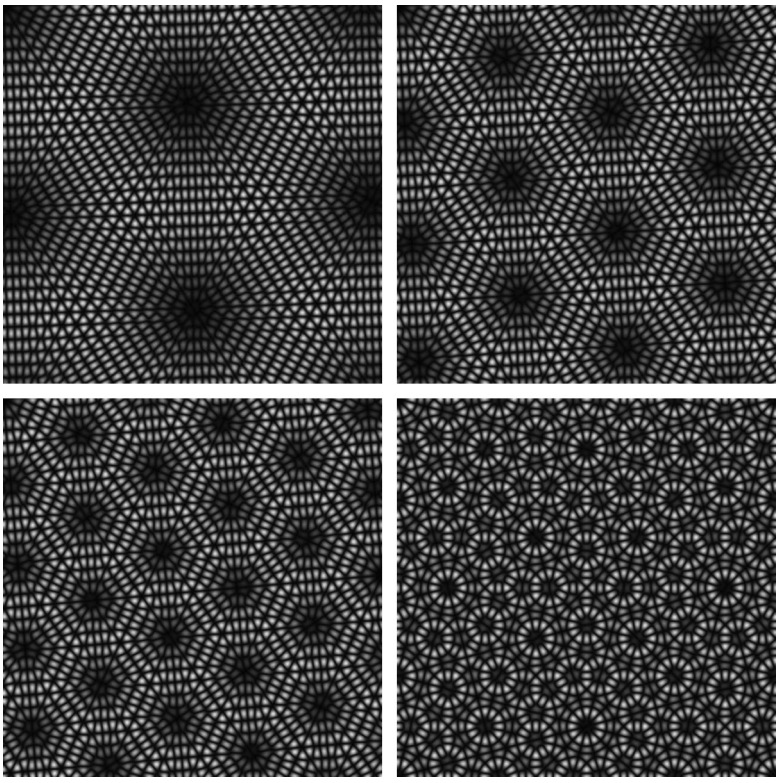

Fig. 4. Superposition of two hexagonal patterns for $\alpha = 4°, 7°, \pi/18, \pi/6$. Order ε and $\beta_1 = -1$ in Theorem 2.5 is represented.

$$\mu_2 = \frac{c}{a} + 3\frac{b}{a}\beta_1^2,\ u_3 = \beta_3 v + \widetilde{u_3},\ \langle \widetilde{u_3}, v\rangle = \langle \widetilde{u_3}, w\rangle = 0$$

The term $\widetilde{u_3}$ only contains Fourier modes $e^{i\,\mathbf{k}\cdot\mathbf{x}}$ with $\mathbf{k} = m_1'\mathbf{k}_1' + m_2'\mathbf{k}_2'$.

Then, we can show easily

(i) $u_{2n} = 0$, $\mu_{2n+1} = 0$, for $n = 1, 2, ...$

(ii) for $\beta_1 = 0$, we recover the classical periodic hexagonal pattern

$$u = \varepsilon\, w + \mathcal{O}(\varepsilon^3),\ \mu = \varepsilon^2\mu_2 + \mathcal{O}(\varepsilon^4),\ \ \mu_2 = 15$$

and using the symmetry $\boldsymbol{\tau}$, the other classical hexagonal pattern

$$\boldsymbol{\tau} u = \varepsilon\, v + \mathcal{O}(\varepsilon^3),\ \mu = \varepsilon^2\mu_2 + \mathcal{O}(\varepsilon^4),\ \mu_2 = 15$$

(iii) For $\beta_1 = \pm 1$, $\mu_2 = 33$ and the series for u and $\boldsymbol{\tau} u = \beta_1 u$ are uniquely determined. Then, the uniqueness of the series implies $\beta_3 = 0$. More generally, at every order, we find u_n orthogonal to the eigenvector v so that finally $\boldsymbol{\tau}\, u(\varepsilon) = \beta_1 u(\varepsilon)$. □

Remark 3. $\mathbf{S}u = -u$ is the solution that corresponds to change ε into $-\varepsilon$, which does not change μ. So, we only have two branches of bifurcating solutions (14) (see Fig. 5).

Remark 4. For $\alpha \in \mathcal{E}_{qp} \cap \mathcal{E}_0$, the proof of existence of a quasipattern with asymptotic expansion (14) is made in [39].

Remark 5. For $\alpha \in \mathcal{E}_p \cap \mathcal{E}_0$, the proof of convergence of the series (14) is standard in the frame of analytical functions of ε (Lyapunov–Schmidt method).

Remark 6. When α is close to 0, it can be shown that the coefficient u_3 is of order $(\alpha)^{-4}$. This is due to $2\,\mathbf{k_j} - \mathbf{k_j'}$ and $2\,\mathbf{k_j'} - \mathbf{k_j}$ occurring as wave vectors, and which have a norm $4(1 - \cos\alpha)$ appearing with a square at the denominator. This factor $(\alpha)^{-4}$ also appears at higher orders in the expansion.

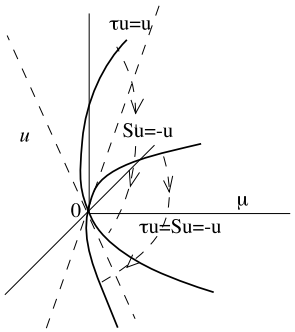

Fig. 5. Bifurcating branches of quasipatterns. Actions of symmetries are indicated with arrows.

3. Concluding remarks

The existence of formal quasipattern solutions to the Swift–Hohenberg equation resulting from two hexagonal patterns has been shown for nearly all values of the angle α. If this result is also true for the Faraday problem, we should ask why no quasipatterns with $\alpha \neq \pi/6$ have been observed in Faraday experiments whereas superlattices have been widely reported. It is possible that it could be difficult to discriminate superlattices and quasipatterns when α is small because of the finite spatial extension of the experiment, but the confusion is not possible as soon as α becomes large enough. An explanation could be that, as in the case of frequency-locked states of two oscillators, nonlinear interactions are able to maintain the locked regime (here the superlattice) on a fairly large window of parameter range. However, borders of superlattice states have been clearly reported in the experiments [35–37]. The neighbor states are hexagons or disordered regimes that involve defects or even spatiotemporal chaos. It is possible that these patterns are more stable than homogeneous quasipatterns. Patterns with defects could be the signature of the transition from superlattices to quasipatterns as shown by Pierre Coullet for one-dimensional spatial patterns [40,41]. A simpler way to handle this problem for superposed hexagonal patterns could be to study the bifurcation to an hexagonal pattern in the presence of a spatial forcing with hexagonal symmetry. This type of problem has been recently reconsidered in crystallography, where the commensurate–incommensurate transition for graphene on a substrate with hexagonal symmetry has been studied [42]. It has been shown that graphene can stretch to adapt to the slightly different periodicity of the substrate and that this depends on the angle between the two hexagonal structures. The transition to an incommensurate state involves defects and domain walls. This problem could be studied using the equation for the slowly varying amplitude of an hexagonal pattern in the presence of a forcing with hexagonal symmetry. This would help understanding how superlattices bifurcate when the mismatch of the pattern with respect to the forcing is increased.

Acknowledgements

We thank Pierre Coullet for helpful discussions and more importantly for all the stimulating collaborations we had together throughout the years.

References

[1] M. Faraday, On the forms and states assumed by fluids in contact with vibrating elastic surfaces, Philos. Trans. R. Soc. Lond. 52 (1831) 319–340.
[2] W. Thomson, Hydrokinetic solutions and observations, Philos. Mag. 42 (1871) 362–377.
[3] H. Bénard, Étude expérimentale du mouvement des liquides propageant la chaleur par convection. Régime permanent : tourbillons cellulaires, C. r. hebd. séances Acad. sci. 130 (1900) 1004–1007;
H. Bénard, Mouvements tourbillonnaires à structure cellulaire. Étude optique de la surface libre, C. r. hebd. séances Acad. sci. 130 (1900) 1065–1068.
[4] S. Chandrasekhar, Hydrodynamic and Hydromagnetic Stability, Clarendon Press, Oxford, 1961.
[5] D. Shechtman, I. Blech, D. Gratias, J.W. Cahn, Metallic phase with long-range orientational order and no translational symmetry, Phys. Rev. Lett. 53 (1984) 1951–1953.
[6] For a review on surface waves, see for instance, S. Fauve, Waves on interfaces, in: H.C. Kuhlmann, H.J. Rath (Eds.), Free Surface Flows, in: CISM Courses and Lectures, vol. 391, 1998, pp. 1–44.
[7] K. Kumar, Linear theory of Faraday instability in viscous liquids, Proc. R. Soc. Lond., Ser. A 452 (1996) 1113.
[8] A.B. Ezerskii, M.I. Rabinovich, V.P. Reutov, I.M. Starobinets, Spatiotemporal chaos in the parametric excitation of a capillary ripple, Sov. Phys. JETP 64 (1986) 1228.
[9] N.B. Tufillaro, R. Ramshankar, J.P. Gollub, Order-disorder transition in capillary ripples, Phys. Rev. Lett. 62 (1989) 422–425.
[10] S. Ciliberto, S. Douady, S. Fauve, Investigating space-time chaos in Faraday instability by means of the fluctuations of the driving acceleration, Europhys. Lett. 15 (1991) 23–28.
[11] S. Fauve, K. Kumar, C. Laroche, D. Beysens, Y. Garrabos, Parametric instability of a liquid-vapor interface close to the critical point, Phys. Rev. Lett. 68 (1992) 3160–3163.
[12] W.S. Edwards, S. Fauve, Patterns and quasi-patterns in the Faraday experiment, J. Fluid Mech. 278 (1994) 123–148.
[13] K. Kumar, K.M.S. Bajaj, Competing patterns in the Faraday experiment, Phys. Rev. E 52 (1995) 4606–4609.
[14] W. Zhang, J. Vinals, Pattern formation in weakly damped parametric surface waves, J. Fluid Mech. 336 (1997) 301–330.

[15] P.L. Chen, J. Vinals, Amplitude equation and pattern selection in Faraday waves, Phys. Rev. E 60 (1999) 559–570.
[16] D. Binks, W. van de Water, Nonlinear pattern formation of Faraday waves, Phys. Rev. Lett. 78 (1997) 4043–4046.
[17] S. Douady, S. Fauve, Pattern selection in Faraday instability, Europhys. Lett. 6 (1988) 221–226.
[18] L. Kahouadji, N. Périnet, L. Tuckerman, S. Shin, J. Chergui, D. Juric, Numerical simulation of supersquare patterns in Faraday waves, J. Fluid Mech. 772 (2015) R2.
[19] W.S. Edwards, S. Fauve, Structure quasicristalline engendrée par instabilité paramétrique, C. R. Acad. Sci. Paris, Ser. II 315 (1992) 417–420.
[20] N.D. Mermin, S.M. Troian, Mean-field theory of quasicrystalline order, Phys. Rev. Lett. 54 (1985) 1524–1527.
[21] For a review, see J. Miles, D. Henderson, Parametrically forced surface waves, Annu. Rev. Fluid Mech. 22 (1990) 143–165 and references therein.
[22] S.T. Milner, Square patterns and secondary instabilities in driven capillary waves, J. Fluid Mech. 225 (1991) 81–100.
[23] N.O. Rojas, M. Argentina, E. Cerda, E. Tirapegui, Inertial lubrication theory, Phys. Rev. Lett. 104 (2010) 187801.
[24] M. Argentina, G. Iooss, Quasipatterns in a parametrically forced horizontal fluid film, Physica D 241 (2012) 1306–1321.
[25] H.W. Muller, Model equations for two-dimensional quasipatterns, Phys. Rev. E 49 (1994) 1273–1277.
[26] R. Lifshitz, D.M. Petrich, Theoretical model for Faraday waves with multiple-frequency forcing, Phys. Rev. Lett. 79 (1997) 1261–1264.
[27] M. Silber, A.C. Skeldon, Parametrically excited surface waves: two-frequency forcing, normal form symmetries, and pattern selection, Phys. Rev. E 59 (1999) 5446–5456.
[28] C.M. Topaz, J. Porter, M. Silber, Multifrequency control of Faraday wave patterns, Phys. Rev. E 70 (2004) 066206.
[29] A.M. Rucklidge, M. Silber, Design of parametrically forced patterns and quasipatterns, SIAM J. Appl. Dyn. Syst. 8 (2009) 298–347.
[30] A.C. Newell, Y. Pomeau, Turbulent crystals in macroscopic systems, J. Phys. A 26 (1993) L429–L434.
[31] A.M. Rucklidge, W.J. Rucklidge, Convergence properties of the 8, 10 and 12 mode representations of quasipatterns, Physica D 178 (2003) 62–82.
[32] G. Iooss, A.M. Rucklidge, On the existence of quasipattern solutions of the Swift–Hohenberg equation, J. Nonlinear Sci. 20 (2010) 361–394.
[33] B. Braaksma, G. Iooss, L. Stolovitch, Existence proof of quasipatterns solutions of the Swift–Hohenberg equation, Commun. Math. Phys. 353 (1) (2017) 37–67, https://doi.org/10.1007/s00220-017-2878-x.
[34] B. Braaksma, G. Iooss, Existence of bifurcating quasipatterns in steady Bénard-Rayleigh convection, Arch. Ration. Mech. Anal. 231 (3) (2019) 1917–1981, https://doi.org/10.1007/s00205-018-1313-6.
[35] A. Kudrolli, B. Pier, J.P. Gollub, Superlattice patterns in surface waves, Physica D 123 (1998) 99–111.
[36] H. Arbell, J. Fineberg, Pattern formation in two-frequency forced parametric waves, Phys. Rev. E 65 (2002) 036224.
[37] T. Epstein, J. Fineberg, Grid states and nonlinear selection in parametrically excited surface waves, Phys. Rev. E 73 (2006) 055302(R).
[38] M. Silber, M.R.E. Proctor, Nonlinear competition between small and large hexagonal patterns, Phys. Rev. Lett. 81 (1998) 2450–2453.
[39] G. Iooss, Existence of quasipatterns in the superposition of two hexagonal patterns, Nonlinearity (2019), to appear.
[40] P. Coullet, Commensurate-incommensurate transition in nonequilibrium systems, Phys. Rev. Lett. 56 (1986) 724–727.
[41] P. Coullet, D. Repaux, Strong resonances of periodic patterns, Europhys. Lett. 3 (1987) 573–579.
[42] C.R. Woods, et al., Commensurate-incommensurate transition in graphene on hexgonal boron nitride, Nat. Phys. 10 (2014) 451–456.